#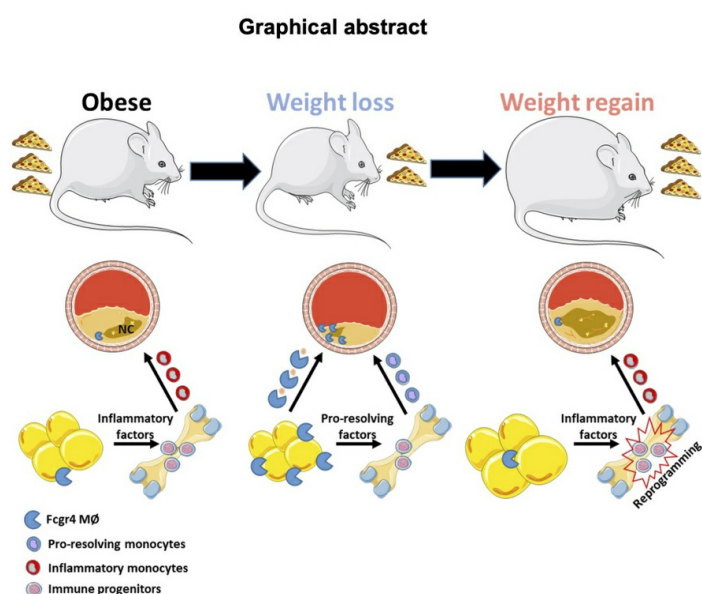 Caloric Restriction Promotes Resolution of Atherosclerosis in Obese Mice, while Weight Regain Accelerates its Progression

Bianca Scolaro, … , Ada Weinstock, Edward A. Fisher

Research   In-Press Preview   Cardiology   Inflammation   Metabolism

Graphical abstract

Caloric Restriction Promotes Resolution of Atherosclerosis in Obese Mice, while Weight Regain Accelerates its Progression

Bianca Scolaro[1], Franziska Krautter[1], Emily J. Brown[1], Aleepta Guha Ray[2], Rotem Kalev-Altman[2], Marie Petitjean[1], Sofie Delbare[1], Casey Donahoe[1], Stephanie Pena[1], Michela L. Garabedian[1], Cyrus A. Nikain[1], Maria Laskou[1], Ozlem Tufanli[1], Carmen Hannemann[1], Myriam Aouadi[3], Ada Weinstock*[2] and Edward A. Fisher*[1]

[1] Department of Medicine, Leon H. Charney Division of Cardiology, Cardiovascular Research Center, New York University Grossman School of Medicine, New York, United States

[2] Department of Medicine, Section of Genetic Medicine, University of Chicago Pritzker School of Medicine, Chicago, United States

[3] Center for Infectious Medicine, Department of Medicine, Karolinska Institute, Huddinge, Sweden

*Address correspondence to either:

Ada Weinstock, 900E 57th Street, room 8122, Chicago, IL, 60601. T: 773-702-2985. adaweinstock@uchicago.edu

Edward A. Fisher, 435 East 30th St., SB705, NY, NY 10016. T: 212-263-6636. edward.fisher@nyulangone.org

Authors declare no conflicts of interest.

ABSTRACT

While weight loss is highly recommended for those with obesity, >60% will regain their lost weight. This weight cycling is associated with elevated risk of cardiovascular disease, relative to never having lost weight. How weight loss/regain *directly* influence atherosclerotic inflammation is unknown. Thus, we studied short-term caloric restriction (stCR) in obese hypercholesterolemic mice, without confounding effects from changes in diet composition. Weight loss was found to promote atherosclerosis resolution independent of plasma cholesterol. From single-cell RNA-sequencing and subsequent mechanistic studies, this can be partly attributed to a unique subset of macrophages accumulating with stCR in epididymal white adipose tissue (eWAT) and atherosclerotic plaques. These macrophages, distinguished by high expression of *Fcgr4*, help to clear necrotic cores in atherosclerotic plaques. Conversely, weight regain (WR) following stCR accelerated atherosclerosis progression with disappearance of *Fcgr4+* macrophages from eWAT and plaques. Furthermore, WR caused reprogramming of immune progenitors, sustaining hyper-inflammatory responsiveness. In summary, we have developed a model to investigate the inflammatory effects of weight cycling on atherosclerosis and the interplay between adipose tissue, bone marrow, and plaques. The findings suggest potential approaches to promote atherosclerosis resolution in obesity and weight cycling through induction of *Fcgr4+* macrophages and inhibition of immune progenitor reprogramming.

INTRODUCTION

Obesity contributes to the establishment and progression of many diseases, including the leading cause of death, atherosclerotic cardiovascular disease (CVD (1, 2)). A major factor thought to underlie this association is the heightened production and release of a variety of potent inflammatory factors (presumably secreted from visceral adipose tissue), such as interleukin (IL)-6, IL-1β, S100A8/9, and TNFα, based on observational studies in humans and mouse models (reviewed in (3)). Contributing to these inflammatory changes are the effects of obesity on insulin resistance and glucose homeostasis. These metabolic perturbations are potent stimulators of local and systemic inflammation through, for example, the production of reactive oxygen species, ligands for the receptor of advanced glycation end-products, and activation of macrophages. In mouse studies, it has also been shown that obesity has effects on hematopoiesis (4). This appears to be through IL-1β secretion from visceral adipose tissue (VAT) macrophages, which is promoted by neighboring adipocytes. This subsequently stimulates the proliferation of bone marrow precursors of monocytes and neutrophils (the major mediators of innate inflammatory responses), thereby increasing their abundance in the circulation and VAT (4).

Sustained weight loss can decrease the risk or severity of many obesity-associated diseases, including CVD (5-7). In addition to improving insulin sensitivity and glucose homeostasis (8), weight loss decreases leukocytosis and inflammatory marker expression associated with obesity (9, 10). Furthermore, weight regain (which occurs in >60% of dieters) increases clinical CVD risk (11) and adipose tissue inflammation in mouse models (12) over what is observed in those never having lost weight. However, cellular and molecular immune mechanisms that facilitate resolution of obesity-related

inflammation with CR and heighten inflammation with weight regain are incompletely known.

To begin addressing these gaps, we previously performed (13) single-cell RNA sequencing (scRNAseq) of epididymal white adipose tissue (eWAT; a surrogate in mice for human VAT) because of the above noted association between this depot and adverse consequences of obesity on inflammation (14). We profiled eWAT leukocytes of mice fed a high-fat high-cholesterol (HFHC) diet to induce obesity before and after short-term (2 weeks) reduction of caloric intake by 30% (13). By maintaining HFHC feeding throughout the study and reducing caloric intake, we achieved weight loss while avoiding confounding the data by inducing epigenetic changes in monocytes and their precursors related to diet compositional changes that result by shifting to chow (15, 16). Our results demonstrated that this type of CR (which we term stCR, for short-term CR) induced a unique immune milieu in the eWAT, neither totally resembling the obese nor the lean landscape.

Most notable was finding an adipose tissue macrophage (ATM) population that accumulates in eWAT with stCR and was characterized by high expression of the IgG antibody receptor *Fcgr4* (in humans, *Fcgr3a*), which promotes phagocytosis (reviewed in (17)). This ATM population expressed many other genes also implicated in phagocytosis, so we hypothesized that these cells assist in clearing apoptotic cells, products of shrinking adipose tissue, and, indeed, there was evidence of this (13). Clearance of apoptotic cells by macrophages (termed efferocytosis) is a critical process in inflammation resolution (18-20), and we hypothesized that stCR induces this process in other macrophage-rich tissues, and thereby promote inflammation resolution beyond that in eWAT (13, 21-26).

Thus, in this report we have focused on effects of stCR on atherosclerotic plaques and extended the results to weight regain.

RESULTS

Short-term caloric restriction in obese mice promotes atherosclerosis resolution

We previously showed in multiple mouse models with hypercholesterolemia that substantial lipid lowering results in the resolution of atherosclerosis as judged by decreased content and inflammatory properties of macrophages (e.g., (24-26)). In order to isolate the effects of weight loss in obesity on established atherosclerosis, a model in which cholesterol levels are not dramatically affected was required. Another consideration in study design was that switching the feeding of a high-fat diet to normal chow results in a severe reduction in food intake (27) (mimicking long-term fasting), as well as in epigenetic changes in macrophages and their precursors related to differences in diet composition (e.g., (15, 16)). Thus, we adapted a protocol of mild stCR(28), keeping the diet composition the same, in order to investigate the role of a clinically relevant level of reduced caloric intake and subsequent weight loss in inflammation resolution in atherosclerosis, independent of cholesterol lowering.

Thus, WT mice were treated with *Ldlr* antisense-oligonucleotide (ASO) to induce LDLr deficiency (as we described previously (29)) and fed a high-fat high-cholesterol (HFHC) diet *ad libitum* for 24 weeks to develop obesity and advanced atherosclerotic plaques. Tissues from the baseline (BL) group (i.e., mice after 24 weeks of HFHC diet) were harvested. To examine early changes induced by weight loss, the stCR group was switched to daily feeding of 70% of their *ad libitum* consumption of the same HFHC diet for an additional 2 weeks (Fig. 1A). The data show that after 24 weeks of treatment, mice were obese, and after 2 weeks of stCR, they lost 14.3% of their weight (Supp. Fig. 1A). Upon harvest, several tissues were weighed and a reduction in eWAT mass was

6

observed (Supp. Fig. 1B) with no significant changes to the masses of inguinal white AT (iWAT), brown AT (BAT), liver or kidney (Supp. Fig. 1C-F).

Examination of metabolic parameters showed marked improvements with stCR, including reduced fasting glucose (Supp. Fig. 1G), lower HOMA-IR (a measure of insulin resistance; Supp. Fig. 1H) and improved glucose tolerance (Supp. Fig. 1I-J). Moreover, plasma cholesterol levels remained elevated after stCR, with non-significant changes between the two groups (Fig. 1B). To investigate the lipoprotein distribution of plasma cholesterol, a subset of plasma samples was fractioned by Fast Protein Liquid Chromatography (FPLC) and cholesterol was measured in each fraction. The results showed no differences in the cholesterol levels in LDL or VLDL fractions between groups. Though HDL cholesterol (HDL-c) was higher in the stCR group by FPLC (Fig. 1C), direct measurements of HDL-c in additional plasma samples showed no difference between BL and stCR mice (Supp. Fig. 1K).

For the evaluation of atherosclerosis, aortic roots were sectioned and investigated for plaque size and composition. While plaque area was comparable between the groups (Supp. Fig. 1L), the stCR group had fewer macrophages, observed both as a decrease in the area of CD68+ cells (Fig. 1D) and their proportion of the total plaque area (Fig. 1E). In an independent analysis, consistent findings were found from digested aortic arches that were analyzed using flow-cytometry. These results showed fewer macrophages in aortic arches of stCR mice, compared to the BL group (Supp. Fig. 1M). To further establish that the changes in the macrophage content of atherosclerotic plaques were independent of plasma cholesterol levels, we investigated whether these parameters were correlated. Statistical analysis shown in Fig. 1F demonstrated no correlation.

7

The change in plaque cellular composition without a decrease in area is reminiscent of several of our previous studies (e.g., (26, 30, 31)), in which inflammation-resolving plaque properties were the predominant feature, with size less significantly affected as the decrease in plaque macrophages was counterbalanced by collagen enrichment, presumably because the content of matrix metalloprotease-producing (inflammatory) macrophages declined. In human plaques, such depletion of macrophages and enrichment in collagen are taken as signs of increased stability (e.g., (32)). To quantify changes in the collagen content of plaques, aortic root sections were stained with picrosirius red and quantified were the positive areas from polarized light images, which represent collagen I, the most common type in atherosclerotic plaques. Indeed, consistent with our previous data, concurrent with decreased plaque macrophages, there was increased collagen content following stCR (Fig. 1G). Representative images of aortic roots stained for CD68 and picrosirius red are presented in Fig. 1H. As alluded to above, these compositional changes to plaques are increasingly appreciated as more clinically relevant than plaque size in terms of the risk of plaque rupture and myocardial infarction (33).

Leukocyte subpopulations in plaques and eWAT dramatically change with stCR

To investigate at the molecular level how stCR influences the immune compartment in atherosclerotic plaques, first, single-cell suspensions were obtained from aortic arches harvested from mice in both experimental groups. CD45+ cells (i.e., all leukocytes) that were viable were sorted and transcripts of individual cells were sequenced, using the 10× Genomics platform (following the method described in (34)). Because we have also obtained adipose tissue CD45+ single-cell transcriptomic data from the same mice (13),

the gene expression profiles from both tissues were merged to identify common subpopulations. Quality control and data filtering are displayed in Supp. Fig. 2A.

Unbiased clustering of the single-cells found 23 distinct clusters (Fig. 2A, Supp. Fig. 2B-D). To annotate the different clusters, we used a published meta-analysis of plaque single-cell transcriptomes as a reference dataset (35) (Supp. Fig. 2C, E). Representative top differentially expressed genes (DEG) in each cluster are presented in Supp. Fig. 2D and Supp. Table 1. Many of the clusters in our dataset corresponded to previously published work (35); however, some clusters not found previously were identified as well. For these, we used our previously published dataset from the eWAT CD45$^+$ cells (Fig. 2A) as the reference dataset (13). Most notable was the appearance of *Fcgr4+* macrophages uniquely in our dataset, which was identified due to their preferential accumulation in stCR conditions. Cell proportions were plotted for each tissue in BL and stCR conditions (Fig. 2B). Note that while all clusters are shared across eWAT and plaques, their distributions considerably differ in both the obese and stCR conditions.

We also investigated whether obesity and stCR drove similar gene expression in *both* eWAT and plaques, as well as in distinct leukocyte clusters within each tissue. The expression of each DEG in eWAT was plotted per leukocyte cluster, and its corresponding expression in plaques is shown in Fig. 2C. We classified all DEGs (columns) as either BL-biased, with log$_2$ fold-change≥1 higher expression in plaque BL (blue), or stCR-biased, with higher log$_2$ fold-change≥1 expression in stCR (red) across all clusters (rows). Many columns (i.e., DEGs) show a signal in multiple rows (cell clusters), indicating that several clusters differentially express the same genes within each tissue, and often in the same direction (either BL or stCR-biased). To look further into this, we plotted the number

of clusters that shared DEGs in each tissue (agnostic of whether they are BL or stCR-biased). Supp. Fig. 2F shows that most changes in gene expression are restricted to a single cell cluster. Numerous genes, however, were differentially expressed in multiple clusters, with some changing coordinately in >15 (Supp. Fig. 2F, Supp. Tables 2-3).

We next investigated whether genes change concordantly (i.e., undergo expression changes in the same direction in response to stCR treatment) *across* tissues (Fig. 2C). For example, macrophages may have changes resulting from their well-known "plasticity" in different tissue environments, but there are also likely to be similarities related to the common origin of these cells from circulating monocytes or their response to treatment. When looking at individual genes (columns) across tissues (top and bottom panels), a number appear to be similarly changing in both eWAT and plaque (as reflected by showing signals in the same columns in the top and bottom plots). This suggests that a core set of genes (Supp. Tables 2-3) is regulated similarly not only between clusters, but also across tissues (e.g., same column in Fig. 2C top and bottom). Most genes, however, appear to be uniquely differentially expressed in one tissue or the other (i.e., not showing concordant signal in Fig. 2C top and bottom), consistent with previous studies (36). Supp. Table 2 summarizes all DEGs shared by 5 or more clusters, further indicating if the expression is BL or stCR biased, and in which tissue.

We also aimed to infer cellular communications between the 23 cell clusters. Ligand-receptor interaction analysis was performed (Methods), and the number of interacting pairs in plaques and eWAT (Supp. Fig. 2G) plotted. The color represents the number of receptor-ligand pairs found between clusters in the X and Y axes. Notably, in both plaque and eWAT, the cells with the highest number of significant ligand-receptor

10

interactions among the leukocytes in both BL and stCR groups are the macrophages (such as Foamy-*Trem2* macrophages and activated macrophages), which mostly communicate with other macrophages (Supp. Fig. 2G). In addition, in eWAT of both BL and stCR groups, there were also predicted interactions of inflammatory macrophages with T cells (CD8+, Treg, and NKT).

To further explore the responses of each macrophage cluster to stCR, the log fold change (LFC) values of DEGs compared to BL were hierarchically clustered and examined for pathway enrichment (Fig. 2D). First, we performed differential expression analysis (see Methods) between stCR and BL within each macrophage cluster, and then calculated LFC values for those genes in all other macrophage clusters. We then performed hierarchical clustering on the LFC values across genes (rows) and macrophage clusters (columns).

There were 8 well-defined gene clusters capturing distinct patterns of differential gene expression across the macrophage clusters. GO and KEGG analyses to assess pathway enrichment in each hierarchical cluster were then performed, and the resulting terms are shown in Fig. 2D. Interestingly, we have previously observed that *Fcgr4+* macrophages accumulate in the eWAT in obese mice following stCR, and they express many genes associated with phagocytosis (13), a process that would be expected to have important functional effects in both tissues. Analysis of plaque macrophage transcriptome changes with stCR indicate that pathways upregulated in *Fcgr4+* macrophages include "Fc-gamma receptor-mediated phagocytosis" and "Regulation of lipolysis in adipocytes" (Fig. 2D). Since *Fcgr4+* macrophages were enriched in both plaque and eWAT with stCR,

we chose to investigate these cells further, and examine whether they play a role in stCR-induced atherosclerosis resolution.

Fcgr4+ macrophages accumulate with weight loss and promote beneficial changes in atherosclerotic plaques

As just noted, in both plaques and eWAT, stCR increased *Fcgr4+* macrophages (Figs. 2B and 3A). These transcriptomic results were verified at the protein level using immunofluorescent staining of aortic roots and eWAT sections for macrophages (CD68 and F4/80, respectively) and FCGR4 (Fig. 3B).

We hypothesized that the functional consequence of the enrichment would be enhanced tissue repair (specifically, inflammation resolution and favorable tissue remodeling), as suggested by Fc-receptors being potent mediators of phagocytosis (reviewed in (17)). Moreover, these macrophages were found to be enriched in other phagocytosis-related genes (13). There is strong rationale for this hypothesis from the recognition in the atherosclerosis field that efferocytosis, or the phagocytosis of dying cells, is an inflammation resolving process that limits the size of plaque necrotic cores (18). Thus, because *Fcgr4* is increased in stCR conditions, we were interested in whether this had a functional consequence on efferocytosis.

To mimic this increase *in vitro*, we measured the efferocytotic activity of macrophages overexpressing the mRNA of the human homologue of *Fcgr4, Fcgr3a.* Control cells were similarly treated with a scrambled mRNA sequence. The cells were used in a standard assay (37) in which macrophages are incubated with fluorescent apoptotic cells, with efferocytotic activity quantified by counting the frequencies of

macrophages that consume apoptotic cells. *Fcgr3a*-overexpressing macrophages had enhanced efferocytotic capacity compared to control cells (Fig. 3C-D), suggesting that the basal level of expression was limiting. To examine whether stCR induces efferocytosis *in vivo*, plaque necrotic core size was assessed in aortic root images, which, as alluded to above, has been shown to inversely correlate with macrophage efferocytotic activity (37, 38). Indeed, the data show smaller necrotic cores in the stCR group (Fig. 3E-G).

To further examine macrophage efferocytotic capacity *in vivo*, plaques were also assessed as described previously (37) for macrophage-associated apoptotic cells (observed as TUNEL+). The results show that compared to BL mice, plaques in the stCR group tended to have more macrophages associated with apoptotic cells (Fig. 3H), again indicative of increased efferocytosis. Notably, we previously reported in eWAT that after stCR, the content of macrophages that had multiple nuclei increased, consistent with their efferocytosis of apoptotic cells (13). Here we found by immunostaining that in both BL and stCR mice, a sizeable proportion of the efferocytes in plaques were FCGR4+, with substantially more efferocytes expressing FCGR4 in the stCR group (33% in BL and 62% in stCR plaques; Fig. 3I-J). It should be remembered that each macrophage performing efferocytosis typically clears several apoptotic cells (37-39). Therefore, even a modest increase in macrophages that have enhanced efferocytotic ability can result in a large increase in dead cell removal, consistent with what we have observed on changes in the necrotic core.

We also investigated whether stCR influences the expression of inflammatory and pro-resolving genes by performing flow-cytometric analysis of plaque macrophages (Supp. Fig. 3A). This revealed that stCR increased the levels of proteins associated with

pro-resolution (e.g., CD163 and CD206) and decreased levels of those associated with inflammation (e.g., Ly6C and CD14). We further tested the response of macrophages overexpressing the human *Fcgr3a* to inflammatory and anti-inflammatory stimuli. To confirm that the *Fcgr3a* overexpression was successful and specific, we measured the expression of the human (*Fcgr3a*) and mouse (*Fcgr4*) genes and found no difference in the expression of *Fcgr4*, but a marked increase in *Fcgr3a* (Fig. 3K). Upon exposure to the inflammatory stimulus lipopolysaccharide (LPS), *Fcgr3a*-overexpressing macrophages showed decreased expression of pro-inflammatory genes, including *Il6, Tnfa* and *Nos2* (Fig. 3K). The response to IL-4 was more diverse, as *Fcgr3a* overexpressing-macrophages enhanced the expression of the pro-resolving gene mannose receptor (*Mrc1*), but not Arginase 1 (*Arg1*) as shown in Fig. 3K.

We sought to further characterize *Fcgr4+* macrophages by performing bulk RNA-sequencing on eWAT macrophages that were either FCGR4+ or negative. For that, obese mice were subjected to stCR, after which single cells from eWAT were isolated. FCGR4 positive and negative macrophages were flow-sorted and their transcriptomes compared. DEGs between macrophages expressing FCGR4 and those not expressing it is presented in Supp. Table 4 and Figure 3L. We found that many genes upregulated in FCGR4+ macrophages are known to be important in the efferocytosis process, such as *Il10* (40) and *Pparg* (41), adding further evidence of their phagocytic/efferocytotic function. We also queried the significantly up and down-regulated genes (adjusted p-value<0.1) of FCGR4+ macrophages for KEGG pathway enrichment (Supp. Fig. 3B). Both "Response to interferon ɣ" and "Antigen processing and presentation" were enriched in the genes from FCGR4+ macrophages, while "Extracellular matrix organization", "Regulation of

angiogenesis", and "Collagen fibril organization" were enriched in the genes with lower expression in FCGR4+ macrophages. Interestingly, genes involved in "Cell killing" were enriched in genes both up- and down-regulated in FCGR4+ macrophages, suggesting that different components of these pathways are at play in FCGR4+ macrophages compared to FCGR4- macrophages.

Taken together, these data suggest that stCR induces a desirable environment in both plaques and eWAT that is associated with decreased expression of inflammatory genes, increased expression of pro-resolving genes and enrichment of *Fcgr4+* macrophages, with these cells promoting clearance of apoptotic cells.

eWAT-derived Fcgr4+ macrophages contribute to the reduction in plaque necrotic core

The data above suggest that cells in the *Fcgr4+* macrophage cluster promote a reduction in plaque necrotic core upon stCR-induced weight loss. Despite being relatively enriched to similar levels in both plaques and eWAT following stCR (Fig. 3A), *Fcgr4+* macrophages, in terms of cell frequency among all leukocytes, constituted a much larger population in eWAT (Fig. 2B and (13)). Thus, we hypothesized that *Fcgr4+* macrophages in eWAT may contribute to resolving atherosclerotic inflammation by inter-organ mechanisms.

To test this hypothesis, we performed adipose tissue transplantation studies, adapting a protocol we previously used (4). Experimentally, 400 mg of eWAT from obese mice pre- or post-stCR were transferred to lean *Ldlr$^{-/-}$* mice with established atherosclerosis (accomplished, as in (42)), by low-fat high-cholesterol diet feeding for 20-weeks to avoid confounding effects of obesity. Because we were focused on assessing

atherosclerosis resolution, mice were transferred to normal chow (with no added cholesterol) to halt disease progression starting 2 days pre-surgery. To investigate trafficking between adipose tissue and atherosclerotic plaques, we incorporated into the protocol eWAT donors with the congenic pan-leukocyte marker CD45.1, and as recipients, CD45.2+ *Ldlr*^{-/-} mice with atherosclerosis (Fig. 4A). Two weeks post-eWAT transplantation, aortae were harvested and examined by flow-cytometry and immunohistochemistry. Single-cell suspensions from aortic arches were analyzed by flow cytometry for leukocyte populations that originated from the transferred eWAT (i.e., CD45.1+).

Approximately 3% of plaque leukocytes are derived from the eWAT in recipients of either obese or stCR eWAT (Supp. Fig. 4A). Despite similar trafficking of ATMs to plaques, there was preferential enrichment of eWAT-derived FCGR4+ macrophages in plaques of recipients of stCR eWAT (Fig. 4B). This might be due in part to changes in macrophage subpopulation abundances in the donor adipose tissue (Fig. 3B), which show increased *Fcgr4*+ macrophages in stCR eWAT.

Recipients of both obese and stCR eWAT had comparable plasma cholesterol levels, which were significantly lower, as expected from the diet change, than BL mice (Supp. Fig. 4B). Histological analyses of aortic root sections showed similar plaque size and macrophage content in recipients of either obese or stCR eWAT (Supp. Fig. 4C-E). Importantly, plaque necrotic cores were smaller in the recipients of the stCR adipose tissue, compared to both BL mice (no adipose transplantation) or recipients of obese adipose tissue (Fig. 4C-E). This suggested that the source of eWAT regulates plaque necrotic core content, with a contribution related to the trafficking of FCGR4+

16

macrophages. This also implies that FCGR4 was not just a marker of cells that accumulate in eWAT with stCR, but a functional factor in the necrotic core improvement.

To directly test this, we knocked down *Fcgr4* expression in eWAT macrophages during the stCR phase. First, WT mice were injected with *Pcsk9*-AAV.8 to induce LDLr deficiency (43) and fed a HFHC diet to promote the development of both atherosclerosis and obesity. After 24 weeks, mice were randomized to have similar average weight/group, and stCR began for 2 weeks. During the stCR phase, mice received daily intraperitoneal injections of glucan-shell particles containing siRNA to *Fcgr4*, or a scrambled sequence as control (Fig. 4F). Note that these particles are preferentially taken up by ATMs when obese mice are injected i.p. (44).

Pilot studies showed that the particles were taken up by 38% of eWAT and 4% of iWAT macrophages, but were not detected in the spleen or bone marrow (Supp. Fig. 4F). *Fcgr4* siRNA-containing particles decreased FCGR4 surface levels in eWAT (Fig. 4G), but not plaque macrophages (Supp. Fig. 4G). Flow-cytometry analysis showed that compared to BL mice, both groups that underwent stCR had more FCGR4+ macrophages in eWAT (Fig. 4H), recapitulating our earlier findings (Fig. 3). Of the eWAT macrophages that were positive for the particles, FCGR4 levels were 32% higher in the control particle treated group compared to the *Fcgr4* siRNA particle-treated mice (Fig. 4G). This corresponded to a 25% decrease in the abundance of eWAT FCGR4+ macrophages in the *Fcgr4* siRNA particle-treated mice (Fig. 4H). Despite this downregulation of FCGR4 compared to the control siRNA treated mice, the *Fcgr4* siRNA particle-treated mice still had significantly higher FCGR4+ macrophages compared to BL (Fig. 4H), likely due to the strong induction by stCR. This suggests that the results of this experiment represent

partial success in suppressing *Fcgr4* mRNA expression and likely underestimate the role of eWAT FCGR4+ macrophages in inflammation resolution.

When examining macrophage and necrotic core content in aortic root sections, we found that plaque size (Supp. Fig. 4H) and macrophage content (Supp. Fig. 4I-J) are similar between the weight loss groups. In contrast, necrotic cores trended to be larger and their proportion of plaque area greater in both BL and recipients of the *Fcgr4* siRNA-containing particles (Fig. 4I-K) compared to control siRNA recipients, despite similar plasma cholesterol levels (Supp. Fig. 4K). Furthermore, there was a negative correlation between the abundance of FCGR4+ macrophages in the plaque or eWAT and plaque necrotic core content (Fig. 4L). These data indicate that elevated FCGR4 levels in eWAT macrophages help to reduce plaque necrotic core, likely related to their greater efferocytotic capacity (Fig. 3 and associated text, above). The reduction in necrotic core might be due to trafficking of FCGR4+ macrophages to plaques (Fig. 4B), or by other mechanisms, such as secreted factors or extra-cellular vesicles originating from these cells (45, 46).

Weight regain accelerates atherosclerosis progression and diminishes the content of Fcgr4+ macrophages in plaques and eWAT

Weight loss that is sustained is beneficial in reducing CV risk (5-7), consistent with the effects of stCR in promoting atherosclerosis inflammation resolution (Figs. 1-4). Weight fluctuation, however, is associated with worsening of CVD compared to the maintenance of an obese state (e.g., (11, 47)). This is an important clinical issue because maintaining weight loss is extremely challenging, with >60% of patients regaining weight (48, 49).

18

To investigate the mechanisms underlying increased CVD with weight fluctuation, we extended the stCR studies to include an additional group of weight regain (WR). For this, $Ldlr^{-/-}$ mice were fed a HFHC diet to establish atherosclerosis and obesity. After 24 weeks, mice were randomized to 4 groups with similar average weights with, once again, the diet composition remaining the same: 1) BL, which was harvested at this time; 2) Progression (PR), which was maintained on *ad libitum* feeding and harvested after an additional 8 weeks; 3) stCR, which was fed 30% fewer calories daily for 2 weeks and then harvested; and, 4) WR, which was put on the stCR regimen identical to group 3 and allowed free access to food thereafter for an additional 6 weeks (Fig. 5A), by which time their weight gain exceeded the BL value (Supp. Fig. 5A). Weights did not significantly differ between the PR and WR groups (Supp Fig. 5B). These feeding regimens did not significantly change plasma cholesterol levels (Supp. Fig. 5C). Additionally, WR promoted marked glucose intolerance (Supp. Fig. 5D-E) and increased the mass of liver, eWAT, iWAT, and BAT compared to BL and stCR mice (Supp. Fig. 5F-I).

We next examined the inflammatory state of plaques. Similar to our previous experiments (Fig. 1D-E), stCR reduced plaque macrophage content compared to BL, while WR plaques contained substantially more macrophages than in the stCR group (Supp. Fig. 5J). To investigate whether WR alters the rate of atherosclerosis progression, we compared the macrophage accumulation rate in plaques of non-weight cycling mice (i.e., from BL to PR) to those that did have weight fluctuation (from stCR to WR). As expected, macrophages gradually accumulated in plaques of mice fed a HFHC diet without weight fluctuation, resulting in an increase in their area by ~33% over 8 weeks. Two weeks of stCR reduced plaque macrophage area by ~28% compared to BL.

Strikingly, WR augmented the macrophage plaque area by ~90% compared to the stCR group (Fig. 5B). Simple linear regression analysis of plaque CD68 area showed a substantial difference in the rates of plaque macrophage accumulation between weight cycling and non-cycling, indicating that WR accelerates atherosclerosis progression.

Because stCR significantly improves several parameters in plaques, WR and PR plaques have different reference points (stCR and BL, respectively). To account for these differences, we also calculated the plaque macrophage fold change, relative to each group's relative baseline (BL for PR and stCR for WR). Notably, these analyses also show that weight cycling results in a more rapid accumulation of macrophages in plaques (Fig. 5C). Moreover, flow-cytometry analysis of aortic arch macrophages revealed that compared to the stCR group, BL and WR plaque macrophages expressed more of the inflammation-associated marker Ly6C and less of the pro-resolving marker CD206 (Supp. Fig. 5K).

Further comparisons between weight cycling and non-cycling showed acceleration of necrotic core formation with weight cycling (Fig. 5D-E). While there was no significant difference in macrophage or necrotic core content between BL and WR after 6 weeks of weight regain, the *rate* of their increases were accelerated in the weight cycling group. Therefore, we postulated that examining these mice at a different timepoint in the weight cycling protocol will show a substantial difference. To test this, we repeated the study only with the PR and WR groups, and harvested the mice at 3 weeks of WR, at the time they regained all their lost weight and had comparable weights to the PR group (Supp. Fig. 5L). Importantly, at this timepoint we also observed a significantly higher CD68 and

necrotic core content in WR plaques compared to non-weight cycled mice (Supp. Fig. 5M-N).

Plaque collagen content, which in human plaques is thought to reflect stability (32), showed the opposite trends to macrophage and necrotic core content: plaques from the stCR group contained significantly more collagen than in the BL or WR group; notably, the collagen gain with stCR was lost with WR (Fig. 5F-G). Representative images of plaques and necrotic cores from BL, stCR and WR are presented in Fig. 5H. Note that in addition to showing that WR accelerates atherosclerosis progression, these data recapitulate our earlier findings that stCR promotes atherosclerosis resolution.

Because *Fcgr4+* macrophage accumulation in plaques and eWAT upon stCR was associated with beneficial changes in both sites, we wondered whether these cells would decrease with WR. To test this, single-cell suspensions were obtained from aortic arches and eWAT, and analyzed by flow cytometry for macrophage FCGR4 levels. The results show, again, that following stCR there were more *Fcgr4+* macrophages in both plaque and eWAT; however, *Fcgr4+* macrophage abundances in both sites reverted to their obese, BL, proportions post-WR (Fig. 5I).

To further characterize the relationship between disease severity and the abundance of FCGR4+ macrophages, we investigated whether there was a correlation between the amount of FCGR4+ macrophages in eWAT or plaques with the content of plaque macrophages or necrotic core. The data show significant inverse correlations between the amount FCGR4+ macrophages in either tissue and plaque necrotic core size (Fig. 5J). A similar correlation tended to be seen (P=0.053) with plaque macrophage content (Supp. Fig. 5O).

Taken together, the results show that WR accelerates atherosclerosis progression, with the plaques displaying rapid expansions of inflammatory cells and necrotic cores, as well as reduced collagen contents, compared to non-weight cycling conditions. Importantly, FCGR4+ macrophage content in either plaques or eWAT inversely correlated with disease severity in WR.

Reprogramming of hematopoietic progenitors by WR has durable adverse effects on atherosclerosis

The data thus far show that stCR reduces, while WR hastens, atherosclerosis. We previously showed that obese eWAT promotes the expansion in bone marrow of immune progenitors with inflammatory potential, resulting in stimulation of myelopoiesis(4). Thus, we hypothesized that weight loss and regain would also influence the production and inflammatory characteristics of immune cells at the level of the bone marrow. To investigate this, the frequencies of bone marrow progenitors (including hematopoietic stem cells; HSC, Lin-Sca-1+cKit+; LSK, multipotent progenitors; MPP, Lin-cKit+; LK, common myeloid progenitors; CMP, granulocyte-monocyte progenitors; GMP and megakaryocyte-erythrocyte progenitors; MEP) and mature circulating leukocytes in the three conditions were determined. Several progenitor populations, including HSCs and MEPs were most abundant in the WR group, while the stCR group had the fewest LK and LSKs (Fig. 6A). This translated in the circulation to lower myeloid (neutrophils, monocytes, eosinophils and basophils), but higher lymphoid cells in the stCR group compared to both BL and WR (Fig. 6B).

Since there was a substantial decrease in leukocytes with stCR, we investigated whether this change can be driven by eWAT. Hence, mice from the adipose transplant studies presented above (Fig. 4A) were analyzed for bone marrow progenitors and mature circulating immune cells. Results show that 2 weeks post-eWAT transplant, there were fewer circulating leukocytes, mainly lymphocytes, in the recipients of the stCR, compared to obese, eWAT (Supp. Fig. 6A). This leukocyte decrease was accompanied by reductions in several hematopoietic progenitor populations in the bone marrow (Supp. Fig. 6B). These data suggest that changes in the eWAT following stCR decrease the inflammatory effects of obese adipose tissue on immune progenitors, which would be expected to contribute to beneficial changes in atherosclerotic plaques (Fig. 4C-E).

Because eWAT from mice undergoing stCR influenced circulating immune cells and their bone marrow progenitors (Supp. Fig. 6A-B), we hypothesized that WR induced innate immune-memory-like changes (also known as trained immunity (50)) in myeloid cells and their precursors that contributed to the deleterious effects on atherosclerosis. To test this, the responses of bone marrow cells from BL, stCR and WR mice to an inflammatory stimulus (LPS) *ex vivo* were examined. Sixteen-hours post-treatment supernatants were assayed for cytokines classically associated with inflammation (IL-6) and its resolution (IL-10). The results show that cells from the stCR group produced the lowest amount of IL-6 and highest amount of IL-10 compared to cells from BL and WR mice (Fig. 6C). The WR cells also produced less IL-6 in response to LPS compared to cells from BL, but more than stCR cells.

To assess whether these alterations in immune responses are influenced specifically by the eWAT, we performed similar *ex vivo* analyses from bone marrow cells

obtained from the fat transplantation study (Fig. 4A). The data show no difference in the production of IL-6, while IL-10 levels trended higher in the group that was transplanted with eWAT from stCR mice (Supp. Fig. 6C). This indicates that the stCR eWAT directly affects the inflammatory status of immune cells and possibly their precursors in the bone marrow by enhancing their production of pro-resolving factors.

Next, we addressed whether these quantitative and qualitative changes to immune cells and their progenitors persist long-term in the context of atherosclerosis and influence plaque properties. To accomplish this, bone marrow transplantation was done, with transfer of cells from the BL, stCR, or WR groups (same mice as in Fig. 5; all CD45.2) to naive, CD45.1 recipients. After recovery from the transplantation, we confirmed substantial bone marrow chimerism with flow-cytometry, using the CD45.1-CD45.2 mismatch (Supp. Fig. 6D). Mice were injected with *Pcsk9*-AAV.8 to induce LDLr-deficiency (25, 43), and began HFHC diet feeding to promote atherosclerosis (Fig. 6D).

After 14 weeks, all bone marrow-recipient mice showed similar glucose tolerance, measured by GTT (area under the curve of 29553+2323 in BL, 27995+1728 in stCR, and 27362+2175 in WR bone marrow recipients). Plasma cholesterol levels were also similar across all groups (Supp. Fig. 6E). Aortic root tissue sections show that, despite no significant differences in plaque size across recipient groups (Supp. Fig. 6F), in recipients of the WR bone marrow, compared to BL and stCR recipients, plaques had more macrophages (Fig. 6E-6F) and larger necrotic cores (Fig. 6G). Although the plaques in the recipients of BL and stCR bone marrow had similar size, macrophage content and necrotic core area, the proportion of necrotic core in plaques was smallest in the stCR recipients (Fig. 6H), which also had the most collagen (as either the absolute area or the

% area of the plaque that was positive; Fig. 6I-6J) compared to both BL and WR. Representative images of plaques are presented in Fig. 6K. Flow-cytometry analysis of aortic arches showed no differences in the proportion of *Fcgr4+* macrophages between the 3 groups (Supp. Fig. 6G). This indicates that bone marrow progenitors do not retain long-term memory to produce *Fcgr4+* macrophages upon cell transfer. This suggests that either transient signals during stCR-induced weight loss promoted their appearance, or that key epigenetic changes in the precursors were not durable, as has been shown in other situations (15, 16).

To verify that the observed changes between weight cycling and non-weight cycling bone marrows are not due to age differences of donors, we repeated the bone marrow transplant study with age-matched PR and WR donors and induced atherosclerosis in naive CD45.1 recipients with *Pcsk9*-AAV.8 (as above). Results of this experiment recapitulated our previous bone marrow transplant experiment: Recipients of bone marrow from WR donors showed several features of exacerbated atherosclerosis, including larger plaques with more macrophages and larger necrotic cores (Supp. Fig. 6H-M).

Examination of bone marrow immune progenitors (Supp. Fig. 6N) and circulating leukocytes (Supp. Fig. 6O) of the study described in Fig. 6D showed no differences in any progenitor or mature cell population across the groups. Although there were no quantitative differences in the number of circulating immune cells and progenitors, we did find that bone marrow cells from WR recipients had increased IL-6 production in response to LPS *ex vivo* (Fig. 6L). Additionally, the stCR bone marrow retained its ability to produce more IL-10 (Fig. 6L), indicating that hematopoietic progenitors preserve some anti-

atherogenic capabilities following stCR, mainly influencing plaque collagen content at 14 weeks of HFHC diet feeding. Taken together, the results suggest that both stCR and WR induce changes in myeloid cells and their precursors that have been seen in other settings (16, 46, 51), particularly the ability to transfer disease-associated phenotypes by bone marrow transplantation.

DISCUSSION

Obesity increases the risk of atherosclerosis-related CVD (52). Observational studies show that sustained weight loss decreases, while weight cycling worsens CVD risk (e.g., (5, 6, 11)). To isolate the effects of weight cycling on atherosclerosis and to gain insights into underlying mechanisms, we devised a mouse model that allows weight fluctuations without confounding effects from changes in plasma cholesterol or diet composition (13). Notable results using the stCR protocol include finding 1) induction of many features of inflammation resolution in atherosclerotic plaques; 2) enrichment in both plaques and eWAT of a macrophage sub-population distinguished by high expression of *Fcgr4*; and, 3) loss of these features when mice were allowed to regain weight after stCR, likely through reprogramming of myeloid progenitors in the bone marrow.

Most studies of weight cycling focus on the effects on systemic metabolism (e.g., glucose intolerance and insulin resistance), and include investigations of adipose tissue (53-55) and the liver (56-58). In this study we investigated concordant changes in eWAT and atherosclerosis with weight fluctuation. Going forward, this mouse model will be a valuable tool to identify further immunological mechanisms that influence atherosclerosis, and possibly other obesity-related co-morbidities in the common situations of weight loss and regain, which is seen in >60% in patients who have dieted (48, 49). Already with a mouse model in which food intake, but not diet composition, is manipulated, we have shown profound short- and long-term changes to the immune compartment and atherosclerosis. The adherence to the same diet composition, with moderate reduction in food intake, is an important distinction of our study compared to others, which involve rounds of diet switching between high-fat and normal chow diets (e.g., (16, 55-60)).

Though some diets were shown to promote epigenetic changes and inflammatory reprogramming in immune precursors (e.g., (15, 16)), it is inherently difficult, if not impossible, to discriminate between the effects of the caloric content, the components of the diets, and plasma lipid levels on the metabolic or immunologic state of the mouse. For instance, Christ et al. showed that Western Diet feeding of $Ldlr^{-/-}$ mice results in inflammatory reprogramming of immune progenitors, even at four weeks after switching to a chow diet that did not result in significant weight loss (15). Recently, Caslin et al. demonstrated that ATMs derived from HFD-fed mice are more inflammatory than from lean ones, a phenotype that was retained after six weeks of normal chow-induced weight loss (55). Yet another example of the confounding effects of changing diet composition and caloric intake at the same time is illustrated by a recent study of a pre-clinical model of macular degeneration, with the exacerbation of disease initially attributed to obesity. In subsequent elegant studies, the causative agent in the diet was identified as stearic acid, suggesting that it was the lower content of this fatty acid in the chow-fed mice, and not their weight loss, that protected them from macular degeneration (16).

In addition to these considerations, there is a fine line separating CR and undernutrition. While the former to a degree is well known to improve health in multiple species, the latter has been shown to promote immune dysfunction (reviewed in (61, 62)). In the first week of diet switch from high-fat diet to normal chow, there is a drastic decrease in food consumption, accounting for ~70% and ~35% reduction in caloric intake compared to HFD and normal chow-fed mice, respectively (55). This dramatic reduction in caloric intake may induce physiological responses that are similar to starvation or malnutrition, rather than the protective responses attributed to CR. Taken together, the

points raised here support the importance in future studies to carefully dissect the differences between various diet regimens to find the most beneficial interventions and their underlying mechanisms.

Our results reveal long-term changes to immune progenitors upon weight loss and regain (Fig. 6). As noted above, recent data indicate that obesity and intermittent Western-Diet feeding promotes inflammatory reprogramming of macrophages (53) and immune progenitors, as well as enhancement of cardiometabolic disease (16, 53, 59, 60). ATMs from previously obese and weight cycling mice (in a model of diet switching from HFD to normal chow) were shown to retain the hyper-inflamed state in response to *ex vivo* stimulations with toll-like receptor ligands (53). Our study is in agreement with the weight cycling, but not the weight loss results. We show that though the weight regain bone marrow cells produce more IL-6 in response to LPS than those from stCR mice, both sources of cells produce less than from obese-derived cells (Fig. 6C). These inconsistencies between studies might be due to the diet regimens, as indicated above, or the different times used as study endpoints. Nonetheless, our data show that weight regain bone marrow produces elevated IL-6 levels even 18 weeks post bone marrow transplantation (Fig. 6L), emphasizing long-term inflammatory effects.

Interestingly, the *in vitro* and *in vivo* data also demonstrate that stCR promotes long term beneficial changes to immune progenitors. *Ex vivo,* bone marrow cells from stCR mice produced more IL-10 (Fig. 6C), even 18 weeks after bone marrow transplant (Fig. 6L). *In vivo*, we see beneficial changes to plaques, mainly reduced necrotic cores and increased collagen contents (Fig. 6H-J), in recipients of stCR bone marrows. This suggests that while weight loss may not necessarily overturn the inflammatory

programming of bone marrow progenitors from obesity, it may induce pro-resolving features. These results further highlight the importance of retaining weight loss, since weight regain induced the most deleterious changes to immune progenitors (Fig. 6E-K, Supp. Fig. 6H-M).

Our data also indicate that the benefits of stCR on atherosclerosis may be attributed, at least in part, to *Fcgr4*+ macrophages. We show that these cells accumulate in both eWAT and plaques upon stCR, but they also disappear with weight regain. Interestingly, the fat transplant studies (Fig. 4) showed evidence of trafficking of *Fcgr4*+ macrophages to the plaque, suggesting this may be yet another mode of inter-organ communication between AT and other tissues (e.g. (63)). The present results further suggest that Fcgr4 at the mRNA and protein levels is not only a marker of macrophages that accumulate with weight loss, but also has functional importance. The expression of *Fcgr4* in eWAT macrophages is inversely associated with plaque necrotic cores, as shown in Fig. 4I-L, with local knockdown of *Fcgr4* in eWAT macrophages impairing the improvements in necrotic cores seen with stCR.

The data further show that overexpression of the human homologue of *Fcgr4* in macrophages enhances their efferocytotic capability (Fig. 3C-D). It is still unknown, however, how FCGR4 regulates efferocytosis beyond its being a receptor that promotes the phagocytosis of immune complexes (64). It is possible, for example, that the expression of *Fcgr4* induces a transcriptional program that facilitates other aspects of efferocytosis. Another possibility is that FCGR4 itself acts as the receptor through which dead cells are being engulfed. If the latter is correct, this will mean that antibody-mediated efferocytosis and macrophage-B cell crosstalk is necessary for this process through

antibody production in B cells and engulfment of opsonized particles via FCGR4 in macrophages. Coating of apoptotic cells by antibodies and their clearance via Fc receptors have been shown in other situations (reviewed in (65)), and we hypothesize this may be a contributing mechanism as well. Future studies will be needed to elucidate these issues. Independent of the possibilities, however, the present data suggest that the basal, or an even lower, level of *Fcgr4* expression is a limiting factor in macrophage efferocytotic activity.

In summary, we have developed a pre-clinical model of weight cycling that avoids confounding effects of concurrent changes in caloric intake and diet composition, and which recapitulates critical CV features reported in human studies. In this model, weight loss induced the appearance of *Fcgr4*+ macrophages in both eWAT and plaque, which help clear plaque necrotic cores likely through their enhanced efferocytosis capabilities. In contrast, CV benefits observed with stCR were lost with weight regain, with the accelerated atherogenesis attributable to durable inflammatory reprogramming of immune progenitors. This acceleration could also be viewed as a "catching up" of the plaque after it regressed to the state achieved by continuous progression. Going forward, the data suggest that *Fcgr4*+ macrophages, as well as innate immune memory, are areas in which to base future interventions to promote the benefits of weight loss and prevent the deleterious effects of weight regain on metabolic inflammation, currently major clinical issues in CVD prevention.

EXPERIMENTAL METHODS

Further information can be found in Supplemental Methods.

SEX AS A BIOLOGICAL VARIABLE

Eight-to-twelve weeks-old male *Ldlr*$^{-/-}$, WT C57BL/6J (CD45.2+) and CD45.1+ mice were used for all experiments, with breeding pairs originally purchased from Jackson Laboratory (Bar Harbor, ME).

Only male mice were used due to female's resistance to develop obesity. Thus, further investigations are needed to determine whether sex-specific differences exist in the response to weight loss and regain.

STUDY APPROVAL

All mouse procedures were approved by the Institutional Animal Care and Use Committee of the New York University School of Medicine.

DATA AVAILABILITY

Data are publicly available in GSE225077 (bulk RNA-seq of *Fcgr4*+ macrophages) and GSE141036 (scRNA-seq of eWAT and plaque leukocytes).

AUTHOR CONTRIBUTIONS

BS, FK, MP, AGR, RKA, CD, SP, MLG, CAN, ML, OT, CH and AW conducted experiments. Conceptualization, study design and supervision were done by AW and EAF. Data analysis was performed by BS, EJB, SD and AW. MA helped with experimental design and provided key reagents. Manuscript was written by BS, EJB, AW and EAF, with edits from all other authors.

REFERENCES

1. Khafagy R, and Dash S. Obesity and Cardiovascular Disease: The Emerging Role of Inflammation. *Front Cardiovasc Med.* 2021;8:768119.
2. Wang Z, and Nakayama T. Inflammation, a link between obesity and cardiovascular disease. *Mediators Inflamm.* 2010;2010:535918.
3. Chait A, and den Hartigh LJ. Adipose Tissue Distribution, Inflammation and Its Metabolic Consequences, Including Diabetes and Cardiovascular Disease. *Front Cardiovasc Med.* 2020;7:22.
4. Nagareddy PR, Kraakman M, Masters SL, Stirzaker RA, Gorman DJ, Grant RW, et al. Adipose tissue macrophages promote myelopoiesis and monocytosis in obesity. *Cell Metab.* 2014;19(5):821-35.
5. Doumouras AG, Wong JA, Paterson JM, Lee Y, Sivapathasundaram B, Tarride JE, et al. Bariatric Surgery and Cardiovascular Outcomes in Patients With Obesity and Cardiovascular Disease:: A Population-Based Retrospective Cohort Study. *Circulation.* 2021;143(15):1468-80.
6. Fisher DP, Johnson E, Haneuse S, Arterburn D, Coleman KJ, O'Connor PJ, et al. Association Between Bariatric Surgery and Macrovascular Disease Outcomes in Patients With Type 2 Diabetes and Severe Obesity. *JAMA.* 2018;320(15):1570-82.
7. Look ARG, Gregg EW, Jakicic JM, Blackburn G, Bloomquist P, Bray GA, et al. Association of the magnitude of weight loss and changes in physical fitness with long-term cardiovascular disease outcomes in overweight or obese people with type 2 diabetes: a post-hoc analysis of the Look AHEAD randomised clinical trial. *Lancet Diabetes Endocrinol.* 2016;4(11):913-21.
8. Sjostrom L, Lindroos AK, Peltonen M, Torgerson J, Bouchard C, Carlsson B, et al. Lifestyle, diabetes, and cardiovascular risk factors 10 years after bariatric surgery. *N Engl J Med.* 2004;351(26):2683-93.
9. Heilbronn LK, Noakes M, and Clifton PM. Energy restriction and weight loss on very-low-fat diets reduce C-reactive protein concentrations in obese, healthy women. *Arterioscler Thromb Vasc Biol.* 2001;21(6):968-70.
10. Lo T, Haridas RS, Rudge EJM, Chase RP, Heshmati K, Lucey EM, et al. Early Changes in Immune Cell Count, Metabolism, and Function Following Sleeve Gastrectomy: A Prospective Human Study. *J Clin Endocrinol Metab.* 2022;107(2):e619-e30.
11. Bangalore S, Fayyad R, Laskey R, DeMicco DA, Messerli FH, and Waters DD. Body-Weight Fluctuations and Outcomes in Coronary Disease. *N Engl J Med.* 2017;376(14):1332-40.
12. Caslin HL, Bhanot M, Bolus WR, and Hasty AH. Adipose tissue macrophages: Unique polarization and bioenergetics in obesity. *Immunol Rev.* 2020;295(1):101-13.
13. Weinstock A, Brown EJ, Garabedian ML, Pena S, Sharma M, Lafaille J, et al. Single-Cell RNA Sequencing of Visceral Adipose Tissue Leukocytes Reveals that Caloric Restriction Following Obesity Promotes the Accumulation of a Distinct Macrophage Population with Features of Phagocytic Cells. *Immunometabolism.* 2019;1.
14. Tchernof A, and Despres JP. Pathophysiology of human visceral obesity: an update. *Physiol Rev.* 2013;93(1):359-404.

15. Christ A, Gunther P, Lauterbach MAR, Duewell P, Biswas D, Pelka K, et al. Western Diet Triggers NLRP3-Dependent Innate Immune Reprogramming. *Cell.* 2018;172(1-2):162-75 e14.

16. Hata M, Andriessen E, Hata M, Diaz-Marin R, Fournier F, Crespo-Garcia S, et al. Past history of obesity triggers persistent epigenetic changes in innate immunity and exacerbates neuroinflammation. *Science.* 2023;379(6627):45-62.

17. Swanson JA, and Hoppe AD. The coordination of signaling during Fc receptor-mediated phagocytosis. *J Leukoc Biol.* 2004;76(6):1093-103.

18. Doran AC, Yurdagul A, Jr., and Tabas I. Efferocytosis in health and disease. *Nat Rev Immunol.* 2020;20(4):254-67.

19. Fullerton JN, and Gilroy DW. Resolution of inflammation: a new therapeutic frontier. *Nat Rev Drug Discov.* 2016;15(8):551-67.

20. Kourtzelis I, Hajishengallis G, and Chavakis T. Phagocytosis of Apoptotic Cells in Resolution of Inflammation. *Front Immunol.* 2020;11:553.

21. Moore KJ, and Tabas I. Macrophages in the pathogenesis of atherosclerosis. *Cell.* 2011;145(3):341-55.

22. Tabas I. Macrophage death and defective inflammation resolution in atherosclerosis. *Nat Rev Immunol.* 2010;10(1):36-46.

23. Yurdagul A, Jr. Metabolic Consequences of Efferocytosis and its Impact on Atherosclerosis. *Immunometabolism.* 2021;3(2).

24. Feig JE, Parathath S, Rong JX, Mick SL, Vengrenyuk Y, Grauer L, et al. Reversal of hyperlipidemia with a genetic switch favorably affects the content and inflammatory state of macrophages in atherosclerotic plaques. *Circulation.* 2011;123(9):989-98.

25. Peled M, Nishi H, Weinstock A, Barrett TJ, Zhou F, Quezada A, et al. A wild-type mouse-based model for the regression of inflammation in atherosclerosis. *PLoS One.* 2017;12(3):e0173975.

26. Weinstock A, Rahman K, Yaacov O, Nishi H, Menon P, Nikain CA, et al. Wnt signaling enhances macrophage responses to IL-4 and promotes resolution of atherosclerosis. *Elife.* 2021;10.

27. Kowalski GM, Hamley S, Selathurai A, Kloehn J, De Souza DP, O'Callaghan S, et al. Reversing diet-induced metabolic dysregulation by diet switching leads to altered hepatic de novo lipogenesis and glycerolipid synthesis. *Sci Rep.* 2016;6:27541.

28. Kosteli A, Sugaru E, Haemmerle G, Martin JF, Lei J, Zechner R, et al. Weight loss and lipolysis promote a dynamic immune response in murine adipose tissue. *J Clin Invest.* 2010;120(10):3466-79.

29. Basu D, Hu Y, Huggins LA, Mullick AE, Graham MJ, Wietecha T, et al. Novel Reversible Model of Atherosclerosis and Regression Using Oligonucleotide Regulation of the LDL Receptor. *Circ Res.* 2018;122(4):560-7.

30. Parathath S, Grauer L, Huang LS, Sanson M, Distel E, Goldberg IJ, et al. Diabetes adversely affects macrophages during atherosclerotic plaque regression in mice. *Diabetes.* 2011;60(6):1759-69.

31. Josefs T, Basu D, Vaisar T, Arets B, Kanter JE, Huggins LA, et al. Atherosclerosis Regression and Cholesterol Efflux in Hypertriglyceridemic Mice. *Circ Res.* 2021;128(6):690-705.

32.   Rekhter MD. Collagen synthesis in atherosclerosis: too much and not enough. *Cardiovasc Res.* 1999;41(2):376-84.

33.   Fuster V, Badimon L, Badimon JJ, and Chesebro JH. The pathogenesis of coronary artery disease and the acute coronary syndromes (1). *N Engl J Med.* 1992;326(4):242-50.

34.   Lin JD, Nishi H, Poles J, Niu X, McCauley C, Rahman K, et al. Single-cell analysis of fate-mapped macrophages reveals heterogeneity, including stem-like properties, during atherosclerosis progression and regression. *JCI Insight.* 2019;4(4).

35.   Zernecke A, Winkels H, Cochain C, Williams JW, Wolf D, Soehnlein O, et al. Meta-Analysis of Leukocyte Diversity in Atherosclerotic Mouse Aortas. *Circ Res.* 2020;127(3):402-26.

36.   Gosselin D, Link VM, Romanoski CE, Fonseca GJ, Eichenfield DZ, Spann NJ, et al. Environment drives selection and function of enhancers controlling tissue-specific macrophage identities. *Cell.* 2014;159(6):1327-40.

37.   Yurdagul A, Jr., Subramanian M, Wang X, Crown SB, Ilkayeva OR, Darville L, et al. Macrophage Metabolism of Apoptotic Cell-Derived Arginine Promotes Continual Efferocytosis and Resolution of Injury. *Cell Metab.* 2020;31(3):518-33 e10.

38.   Yurdagul A, Jr., Doran AC, Cai B, Fredman G, and Tabas IA. Mechanisms and Consequences of Defective Efferocytosis in Atherosclerosis. *Front Cardiovasc Med.* 2017;4:86.

39.   Tufan T, Comertpay G, Villani A, Nelson GM, Terekhova M, Kelley S, et al. Rapid unleashing of macrophage efferocytic capacity via transcriptional pause release. *Nature.* 2024;628(8007):408-15.

40.   Proto JD, Doran AC, Gusarova G, Yurdagul A, Jr., Sozen E, Subramanian M, et al. Regulatory T Cells Promote Macrophage Efferocytosis during Inflammation Resolution. *Immunity.* 2018;49(4):666-77 e6.

41.   Yoon YS, Kim SY, Kim MJ, Lim JH, Cho MS, and Kang JL. PPARgamma activation following apoptotic cell instillation promotes resolution of lung inflammation and fibrosis via regulation of efferocytosis and proresolving cytokines. *Mucosal Immunol.* 2015;8(5):1031-46.

42.   Hartvigsen K, Binder CJ, Hansen LF, Rafia A, Juliano J, Horkko S, et al. A diet-induced hypercholesterolemic murine model to study atherogenesis without obesity and metabolic syndrome. *Arterioscler Thromb Vasc Biol.* 2007;27(4):878-85.

43.   Bjorklund MM, Hollensen AK, Hagensen MK, Dagnaes-Hansen F, Christoffersen C, Mikkelsen JG, et al. Induction of atherosclerosis in mice and hamsters without germline genetic engineering. *Circ Res.* 2014;114(11):1684-9.

44.   Aouadi M, Tencerova M, Vangala P, Yawe JC, Nicoloro SM, Amano SU, et al. Gene silencing in adipose tissue macrophages regulates whole-body metabolism in obese mice. *Proc Natl Acad Sci U S A.* 2013;110(20):8278-83.

45.   Kita S, Maeda N, and Shimomura I. Interorgan communication by exosomes, adipose tissue, and adiponectin in metabolic syndrome. *J Clin Invest.* 2019;129(10):4041-9.

46.   Kahn CR, Wang G, and Lee KY. Altered adipose tissue and adipocyte function in the pathogenesis of metabolic syndrome. *J Clin Invest.* 2019;129(10):3990-4000.

47.   Kaze AD, Santhanam P, Erqou S, Ahima RS, Bertoni AG, and Echouffo-Tcheugui JB. Body Weight Variability and Risk of Cardiovascular Outcomes and Death in the Context of

Weight Loss Intervention Among Patients With Type 2 Diabetes. *JAMA Netw Open.* 2022;5(2):e220055.

48. Fildes A, Charlton J, Rudisill C, Littlejohns P, Prevost AT, and Gulliford MC. Probability of an Obese Person Attaining Normal Body Weight: Cohort Study Using Electronic Health Records. *Am J Public Health.* 2015;105(9):e54-9.

49. Wing RR, and Phelan S. Long-term weight loss maintenance. *Am J Clin Nutr.* 2005;82(1 Suppl):222S-5S.

50. Netea MG, Dominguez-Andres J, Barreiro LB, Chavakis T, Divangahi M, Fuchs E, et al. Defining trained immunity and its role in health and disease. *Nat Rev Immunol.* 2020;20(6):375-88.

51. Priem B, van Leent MMT, Teunissen AJP, Sofias AM, Mourits VP, Willemsen L, et al. Trained Immunity-Promoting Nanobiologic Therapy Suppresses Tumor Growth and Potentiates Checkpoint Inhibition. *Cell.* 2020;183(3):786-801 e19.

52. Powell-Wiley TM, Poirier P, Burke LE, Despres JP, Gordon-Larsen P, Lavie CJ, et al. Obesity and Cardiovascular Disease: A Scientific Statement From the American Heart Association. *Circulation.* 2021;143(21):e984-e1010.

53. Caslin HL, Cottam MA, Pinon JM, Boney LY, and Hasty AH. Weight cycling induces innate immune memory in adipose tissue macrophages. *Front Immunol.* 2022;13:984859.

54. Barbosa-da-Silva S, Fraulob-Aquino JC, Lopes JR, Mandarim-de-Lacerda CA, and Aguila MB. Weight cycling enhances adipose tissue inflammatory responses in male mice. *PLoS One.* 2012;7(7):e39837.

55. Cottam MA, Caslin HL, Winn NC, and Hasty AH. Multiomics reveals persistence of obesity-associated immune cell phenotypes in adipose tissue during weight loss and weight regain in mice. *Nat Commun.* 2022;13(1):2950.

56. Barbosa-da-Silva S, da Silva NC, Aguila MB, and Mandarim-de-Lacerda CA. Liver damage is not reversed during the lean period in diet-induced weight cycling in mice. *Hepatol Res.* 2014;44(4):450-9.

57. Vatarescu M, Bechor S, Haim Y, Pecht T, Tarnovscki T, Slutsky N, et al. Adipose tissue supports normalization of macrophage and liver lipid handling in obesity reversal. *J Endocrinol.* 2017;233(3):293-305.

58. Zamarron BF, Porsche CE, Luan D, Lucas HR, Mergian TA, Martinez-Santibanez G, et al. Weight Regain in Formerly Obese Mice Hastens Development of Hepatic Steatosis Due to Impaired Adipose Tissue Function. *Obesity (Silver Spring).* 2020;28(6):1086-97.

59. Takaoka M, Zhao X, Lim HY, Magnussen CG, Ang O, Suffee N, et al. Early intermittent hyperlipidaemia alters tissue macrophages to fuel atherosclerosis. *Nature.* 2024;634(8033):457-65.

60. Lavillegrand JR, Al-Rifai R, Thietart S, Guyon T, Vandestienne M, Cohen R, et al. Alternating high-fat diet enhances atherosclerosis by neutrophil reprogramming. *Nature.* 2024;634(8033):447-56.

61. Bourke CD, Berkley JA, and Prendergast AJ. Immune Dysfunction as a Cause and Consequence of Malnutrition. *Trends Immunol.* 2016;37(6):386-98.

62. Collins N, and Belkaid Y. Control of immunity via nutritional interventions. *Immunity.* 2022;55(2):210-23.

63. Funcke JB, and Scherer PE. Beyond adiponectin and leptin: adipose tissue-derived mediators of inter-organ communication. *J Lipid Res.* 2019;60(10):1648-84.

64. Nimmerjahn F, and Ravetch JV. Antibody-mediated modulation of immune responses. *Immunol Rev.* 2010;236:265-75.

65. Cockram TOJ, Dundee JM, Popescu AS, and Brown GC. The Phagocytic Code Regulating Phagocytosis of Mammalian Cells. *Front Immunol.* 2021;12:629979.
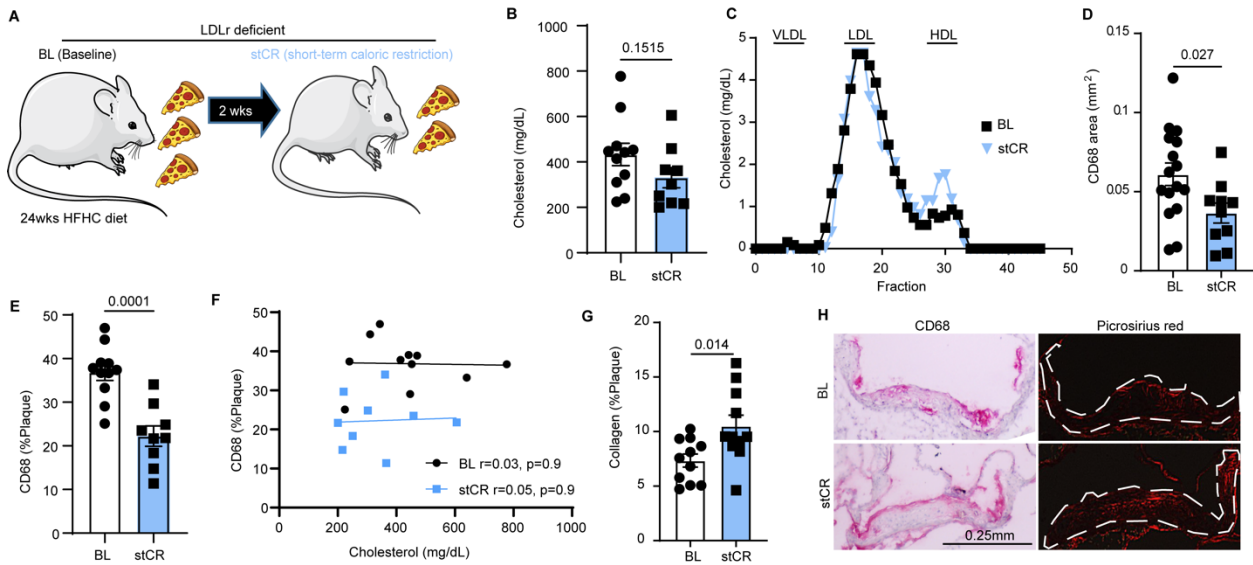
Figure 1

Fig. 1: stCR induces atherosclerosis resolution.

(A) Experimental design. WT mice were fed a high-fat, high-cholesterol (HFHC) diet and treated with LDLr antisense oligonucleotide for 24 weeks to induce obesity and atherosclerosis (baseline or BL group). Mice were then calorically restricted for 2 weeks, by reducing food intake by 30% (n=12-14; short term caloric restriction or stCR group). (B) Plasma cholesterol levels and (C) lipoprotein profile at the end of the experiment. Quantification in (C) was performed on pooled plasma from 3 mice/group. (D, E) Plaque macrophage content quantified through CD68 staining. (F) Simple linear regression showing lack of correlation between cholesterol levels and CD68 content in plaques. (G) Collagen quantification in plaques assessed through Picrosirius red staining. (H) Representative aortic root images. P-values were determined via two-tailed Student's t-test.
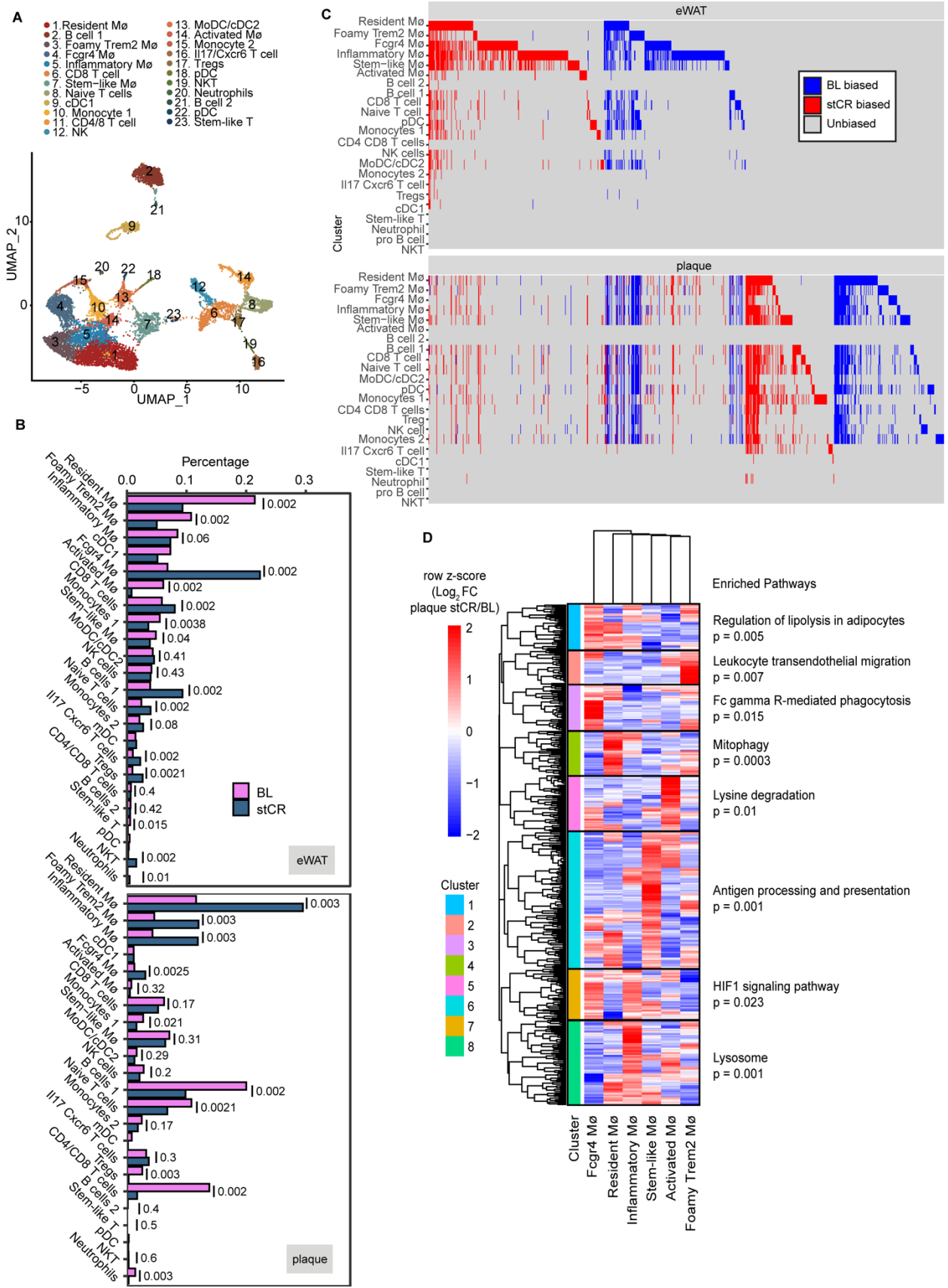
Fig. 2: The immune landscape in plaque and eWAT changes with stCR.

(A) Unbiased clustering of scRNAseq dataset represented in an UMAP. (B) Proportion of each cell cluster identified in the scRNAseq analysis. (C) Genes (columns) differentially expressed in stCR compared to BL are plotted per cluster (rows) in epididymal white adipose tissue (eWAT; top) and plaque (bottom). In blue and red are genes that are upregulated in BL and stCR, respectively, or unchanged in grey. All DEGs have adjusted p-value < 0.1. Bias to stCR in eWAT indicates $\log_2(stCR/BL) > 0$; bias to BL in eWAT indicates $\log_2(stCR/BL) < 0$; bias to stCR in plaque indicates $\log_2(stCR/BL) > 1$; bias to BL in plaque indicates $\log_2(stCR/BL) < -1$. (D) Hierarchical clustering of differentially expressed genes (DEGs) in all macrophage clusters of the scRNAseq dataset, and their associated enriched pathways. Values in the heatmap show row Z-scores of $\log_2(stCR/BL)$ in plaque.
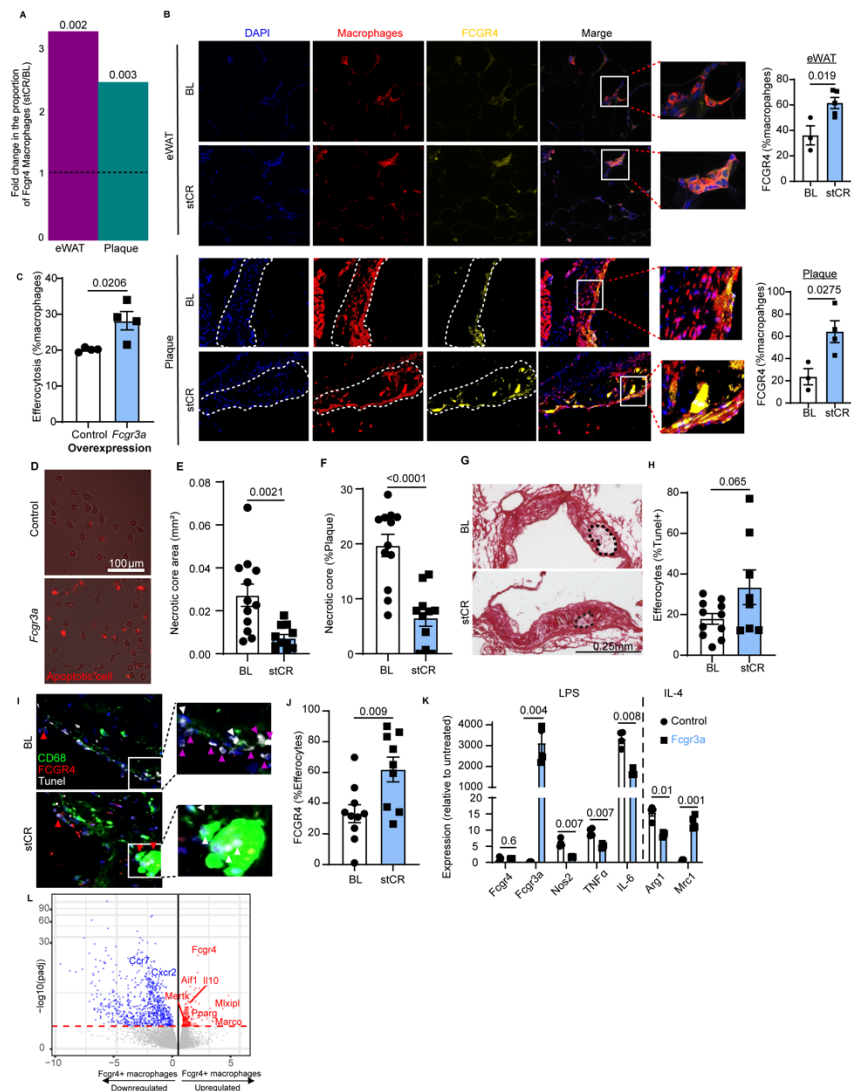
Fig. 3: FCGR4 positive macrophages accumulate with weight loss and promote a pro-reparative phenotype and increased efferocytosis.

(A) Fold change in the proportion of *Fcgr4+* macrophages in stCR mice, compared to baseline, in plaque and eWAT, quantified from the scRNAseq data. Dotted line indicates the baseline levels, and p-values (on top of bars) for the differences from baseline were determined using false-discovery rate. (B) Images and quantification of FCGR4 and macrophage staining in eWAT and aortic roots (n=3-5). (C, D) Human *Fcgr3a* mRNA, or

a scrambled sequence as control, was introduced to BMDMs. After 24 hours, macrophages were exposed to fluorescently labeled apoptotic macrophages. Efferocytotic events were determined as macrophages having an attached or engulfed red label. (E-G) Plaque necrotic core quantification in root sections of baseline and stCR mice presented in Fig. 1 (n=11-12). (H-J) In situ efferocytosis assay of aortic root sections in which (I) apoptotic cells were labeled by TUNEL (white), macrophages by anti-CD68 (green), FCGR4 (red) and nuclei by DAPI (blue). White arrows indicate macrophage-associated TUNEL, purple arrow mark free TUNEL, and red arrows point to Fcgr4+ macrophages associated with TUNEL. Efferocytosis was calculated as (H) total efferocytes (TUNEL+ macrophages) and as (J) FCGR4+, TUNEL+ macrophages. (K) Gene expression of inflammatory (*Nos2, Il6* and *Tnfa*) and anti-inflammatory (*Mrc1* and *Arg1*) markers following LPS or IL-4 stimulation, respectively, of control or *Fcgr3a* overexpressing macrophages (n=4). (L) Volcano plot showing DE genes in FCGR4+, compared to FCGR- macrophages from eWAT following stCR. P-values were determined by two-tailed Student's t-test.
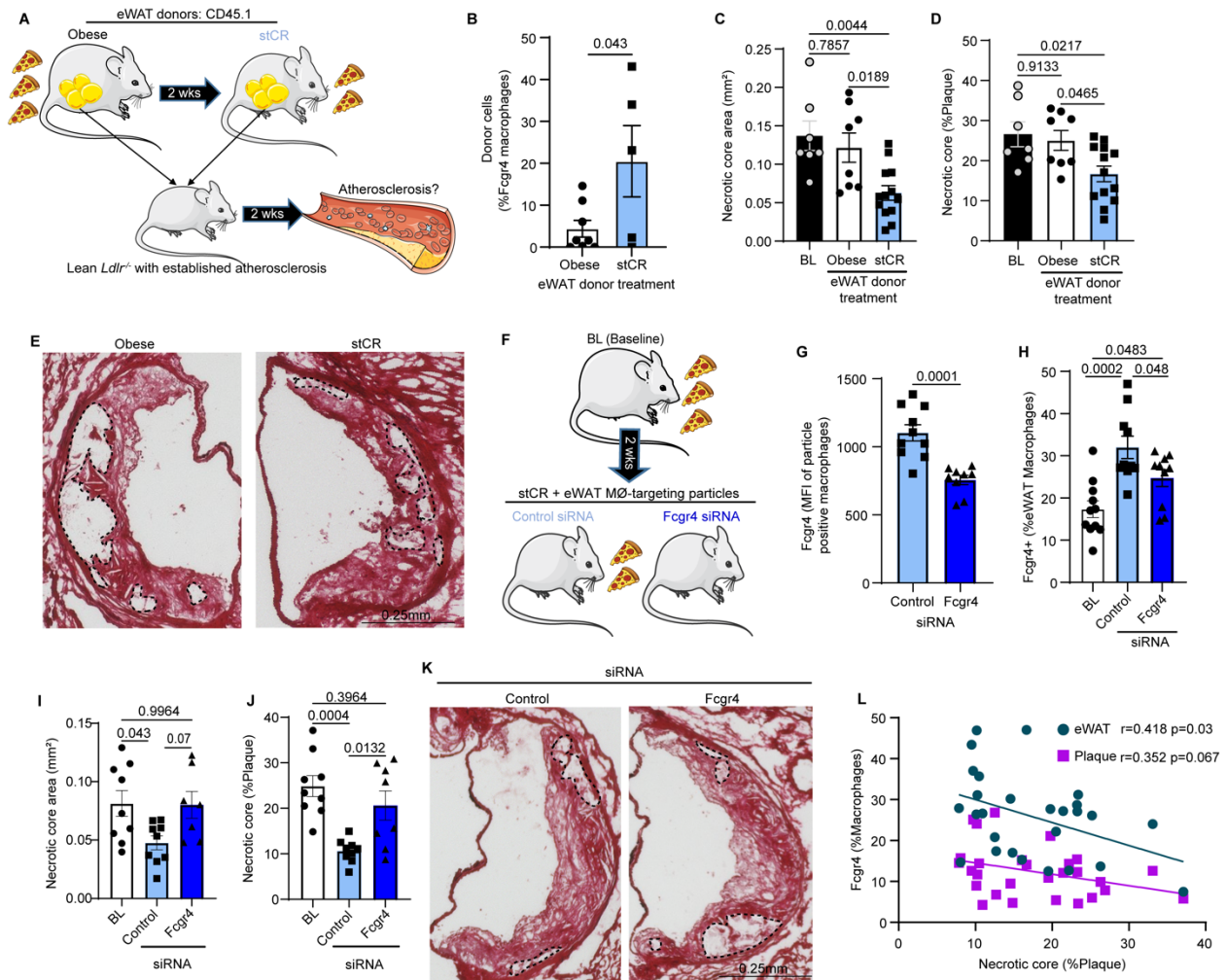
Fig. 4: eWAT-derived *Fcgr4*+ macrophages reduce plaque necrotic core.

(A) Schematic of adipose tissue transplantation experiment (n=7-12). (B) Presence of

FCGR4+ macrophages derived from donor adipose tissue in plaques of recipient mice,

determined by flow cytometry (n=5-6). (C, D) Plaque necrotic core quantification in root

sections of eWAT recipients, according to donor's group treatment, with (E)

representative images. (F) Experimental design of knockdown of *Fcgr4* in eWAT

macrophages during stCR (n=7-10). Flow cytometry analysis after injection of control or

Fcgr4 siRNA particles of (G) FCGR4 surface expression in eWAT macrophages, and

(H) FCGR4+ macrophages as % of total eWAT macrophages. (I, J) Plaque necrotic

core quantification in root sections, with (K) representative images. (L) Simple linear regression showing correlation between *Fcgr4+* macrophages and necrotic core. P-values were determined via (B, H) two-tailed Student's t-test (C, D, G, I, J) one-way ANOVA with Tukey's multiple comparisons test and (L) simple linear regression analysis.
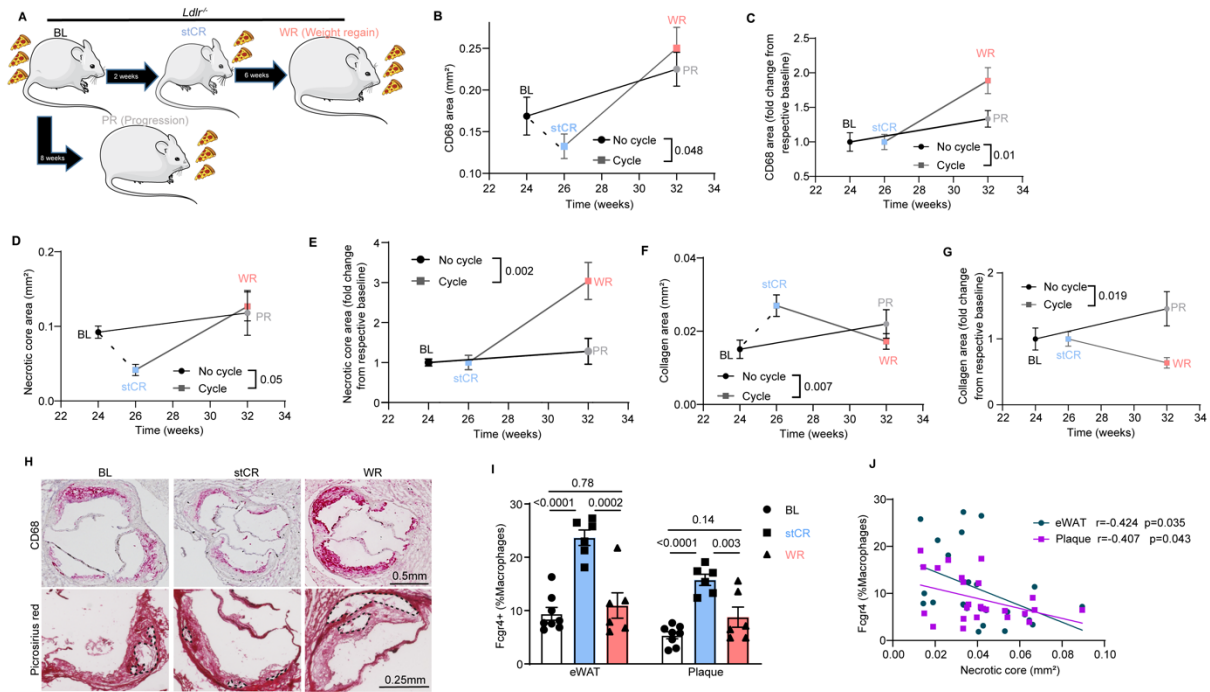
Fig 5: Weight regain reverts _Fcgr4_+ macrophage levels to obese proportions and accelerates atherosclerosis progression.

(A) Schematic of weight regain experiment. Weight regain (WR) was induced by allowing ad libitum access to HFHC diet after a two-week weight loss period achieved by stCR. Mice in the progression group (PR) were allowed to continue to eat ad libitum after the BL time point. (B-G) Rates of change in plaque (B-C) macrophages, (D-E) necrotic core and (F-G) collagen areas in weight cycling vs. non-cycling. Data are expressed as (B, D, F) absolute area and (C, E, G) change from respective baseline (BL for PR and stCR for WR), n=11-15. (H) Representative aortic root images. (I) Flow cytometry analysis of FCGR4+ macrophages in eWAT and plaques (n=6). (J) Simple linear regression showing correlation between _Fcgr4_+ macrophages from eWAT and plaques with plaque necrotic core. P-values were determined via (B-G, J) simple linear regression and (I) one-way ANOVA with Tukey's multiple comparisons test.
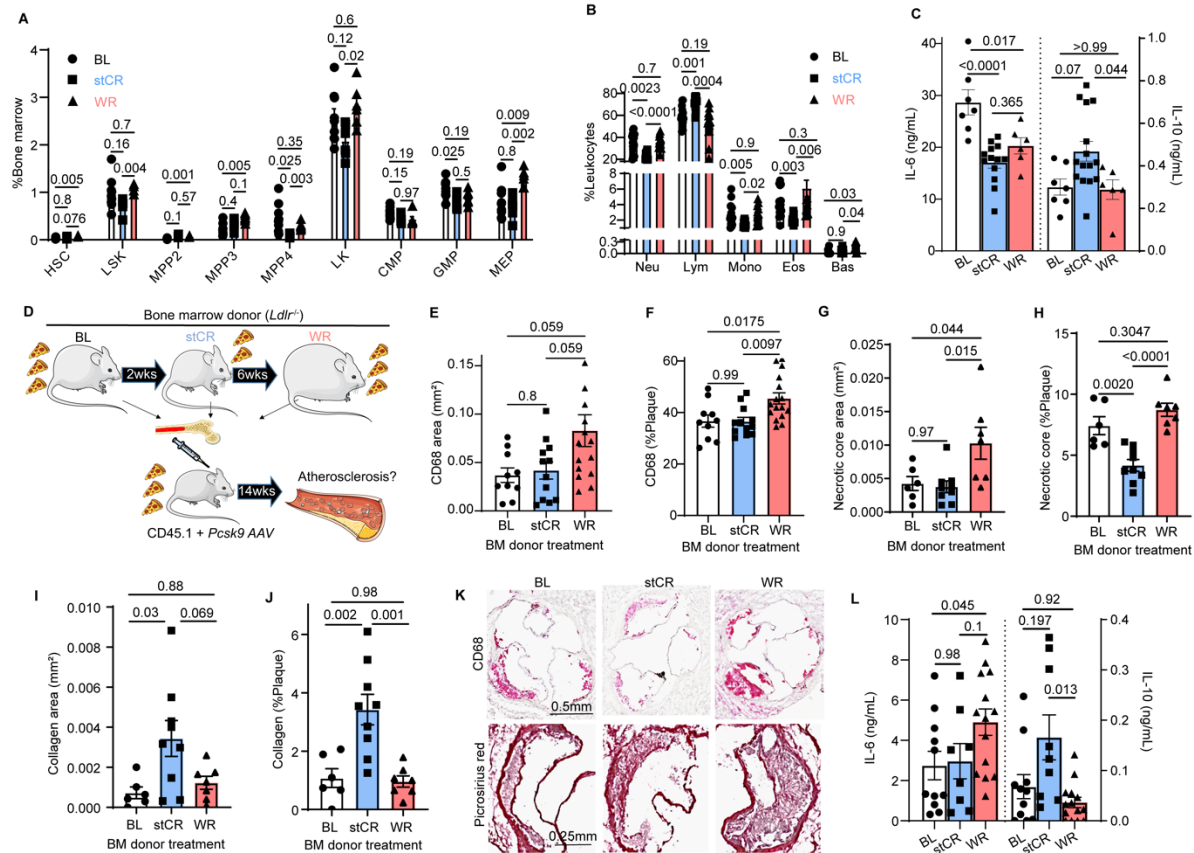
Fig 6: Weight regain induces long-term pro-atherogenic reprogramming of hematopoietic progenitors.

(A) Frequencies of bone marrow hematopoietic stem and progenitor cells (n=6-9) and

(B) circulating white blood cells (n=13-17) in weight loss and regain mice (from Fig. 5).

(C) Cytokines produced by bone marrow cells treated *ex vivo* with LPS for 16h. (D)

Schematic of bone marrow transplantation experiment (n=10-14). (E) Plaque

macrophage content expressed as total area and (F) percent of plaque area assessed

by CD68 staining in aortic roots after 14 weeks of HFHC diet. (G, H) Plaque necrotic

core and (I, J) collagen quantifications in root sections, with (K) representative images.

(L) Cytokines secreted by bone marrow cells isolated from bone marrow recipient mice

and treated ex vivo with LPS for 16h. P-values were determined via (A-B) two-way

ANOVA and (C-L) one-way ANOVA with Tukey's multiple comparisons test.